



Title	Rab8b Regulates Transport of West Nile Virus Particles from Recycling Endosomes
Author(s)	Kobayashi, Shintaro; Suzuki, Tadaki; Kawaguchi, Akira; Phongphaew, Wallaya; Yoshii, Kentaro; Iwano, Tomohiko; Harada, Akihiro; Kariwa, Hiroaki; Orba, Yasuko; Sawa, Hirofumi
Citation	Journal of Biological Chemistry (JBC), 291(12), 6559-6568 <a href="https://doi.org/10.1074/jbc.M115.712760">https://doi.org/10.1074/jbc.M115.712760</a>
Issue Date	2016-03-18
Doc URL	<a href="http://hdl.handle.net/2115/62049">http://hdl.handle.net/2115/62049</a>
Rights	This research was originally published in Journal of Biological Chemistry. Shintaro Kobayashi, Tadaki Suzuki, Akira Kawaguchi, Wallaya Phongphaew, Kentaro Yoshii, Tomohiko Iwano, Akihiro Harada, Hiroaki Kariwa, Yasuko Orba and Hirofumi Sawa. Rab8b Regulates Transport of West Nile Virus Particles from Recycling Endosomes. The Journal of Biological Chemistry. 2016; 291(12): 6559-6568. © the American Society for Biochemistry and Molecular Biology.
Type	article (author version)
File Information	JBC 291 (12)p.6559-6568.pdf



[Instructions for use](#)

Rab8b Regulates Transport of West Nile Virus Particles from Recycling Endosomes

**Shintaro Kobayashi<sup>1,2</sup>, Tadaki Suzuki<sup>3</sup>, Akira Kawaguchi<sup>1</sup>, Wallaya Phongphaew<sup>1</sup>, Kentaro Yoshii<sup>2</sup>, Tomohiko Iwano<sup>4</sup>, Akihiro Harada<sup>5</sup>, Hiroaki Kariwa<sup>2</sup>, Yasuko Orba<sup>1</sup>, and Hirofumi Sawa<sup>1,6</sup>**

<sup>1</sup> From the Division of Molecular Pathobiology, Research Center for Zoonosis Control, Hokkaido University, N20, W10, Kita-ku, Sapporo 001-0020, Japan

<sup>2</sup> Laboratory of Public Health, Graduate School of Veterinary Medicine, Hokkaido University, N18, W9, Kita-ku, Sapporo 060-0818, Japan

<sup>3</sup> Department of Pathology, National Institute of Infectious Diseases, 1-23-1 Toyama, Shinjuku-Ku, Tokyo 162-8640, Japan

<sup>4</sup> Department of Anatomy and Cell Biology, Interdisciplinary Graduate School of Medicine and Engineering, University of Yamanashi, 1110 Shimo-Kateau, Chuo, Yamanashi 409-3898, Japan

<sup>5</sup> Department of Cell Biology, Graduate School of Medicine, Osaka University, 2-2 Yamadaoka, Suita, Osaka 565-0871, Japan

<sup>6</sup> Global Institution for Collaborative Research and Education (GI-CoRE), Hokkaido University, N20, W10, Kita-ku, Sapporo 001-0020, Japan

\*Running title: *Rab8b plays a role in WNV particle release*

To whom correspondence should be addressed: Hirofumi Sawa, Division of Molecular Pathobiology, Research Center for Zoonosis Control, Hokkaido University, N20, W10, Kita-ku, Sapporo 001-0020, Japan, Tel.: +81-11-706-5185; Fax: +81-11-706-7370; E-mail: h-sawa@czc.hokudai.ac.jp

**Keywords:** Rab / vesicles / transport / Flavivirus / infection

## ABSTRACT

West Nile virus (WNV) particles assemble at and bud into the endoplasmic reticulum (ER) and are secreted from infected cells through the secretory pathway. However, the host factor related to these steps is not fully understood. Rab proteins, belonging to the Ras superfamily, play essential roles in regulating many aspects of vesicular trafficking. In this study, we sought to determine which Rab proteins are involved in intracellular trafficking of nascent WNV particles. RNAi analysis revealed that Rab8b plays a role in WNV particle release. We found that Rab8 and WNV antigen were colocalized in WNV-infected human neuroblastoma cells, and that WNV infection enhanced Rab8 expression in the cells. In addition, the amount of WNV particles in the supernatant of Rab8b-deficient cells was significantly decreased compared with that of wild-type cells. We also demonstrated that WNV particles accumulated in

the recycling endosomes in WNV-infected cells. In summary, these results suggest that Rab8b is involved in trafficking of WNV particles from recycling endosomes to the plasma membrane.

## INTRODUCTION

Viruses have many strategies to exploit the host cellular machinery and evade recognition of host defenses for their replication. They utilize host machinery to promote their entry, replication and release.

West Nile virus (WNV) is an enveloped, single-stranded, positive-sense RNA virus belonging to the *Flaviviridae* family. In nature, WNV circulates between mosquitoes and birds, and humans and other mammals are incidental hosts (1). In humans, WNV causes a febrile illness, with a subset of patients progressing to severe neurological disease (2). WNV enters host cells through unknown cell surface receptor-mediated

endocytosis and is transported to endosomes (3), followed by endosomal membrane fusion and delivery of the infectious RNA genome into the cytoplasm (4,5). The viral genome is translated as a single polyprotein that is cleaved by host and viral proteases into three structural (C, prM and E) and seven nonstructural (NS1, NS2A, NS2B, NS3, NS4A, NS4B and NS5) proteins (4,5). The structural proteins are components of viral particles and the nonstructural proteins form the replication complex that is essential for replication of viral RNA (6,7). The viral particles assemble and bud into the ER to form immature particles (8). Viral particle maturation takes place in the Golgi and acidic compartments during transport through the host secretory pathway, and mature particles are released by exocytosis (9,10). The release of WNV particles through the secretory pathway is well documented; however, little is known about detailed trafficking pathways and related host factors used to deliver the newly formed viral particles to the plasma membrane.

Members of the Rab family of small GTPases regulate intracellular membrane traffic. More than 60 known Rab proteins are localized to each different intracellular organelle on both the endocytic and exocytic pathways of eukaryotic cells (11). Rab proteins recruit and interact with effector proteins, either directly or indirectly, to target vesicles to the appropriate sites on acceptor membranes (12). Several Rab proteins are involved in the life cycles of various enveloped viruses, including WNV (13,14). WNV replication is hampered in cells transfected with siRNA of Rab5, suggesting that a Rab5-dependent endocytosis pathway is important for WNV entry (14). Thus, many Rab proteins seem to be involved in WNV infection, but their role in secretion of WNV particles is not well elucidated.

Advances in genomics and RNAi methods have led to genome-wide screening to identify the cellular genes that affect viral replication (15,16). There are several reports of WNV virus-like particles (VLPs), which are produced by complementation of replicon RNA with WNV structural genes expressed *in trans* (17), for the screening of siRNA or compound libraries (18,19). In this study, we performed siRNA-based screen silencing of Rab proteins related to vesicle transport from the ER to the plasma membrane to elucidate the mechanisms of WNV particle release.

We found that Rab8b is important for WNV particle release and defective Rab8b results in accumulation of WNV particles in recycling endosomes.

## **EXPERIMENTAL PROCEDURES**

**Cells and virus** – HEK-293T cells were grown in high-glucose DMEM (Sigma, St. Louis, MO) supplemented with 10% heat-inactivated FBS. Vero cells were grown in minimal essential medium (MEM; Nissui, Tokyo, Japan) supplemented with 10% heat-inactivated FBS and 2 mM L-glutamine (Sigma). SH-SY5Y cells were grown in DMEM/Nutrient Mixture F-12 Ham (Sigma) supplemented with 10% heat-inactivated FBS. WT, Rab8b KO and Rab8a/b double knockout (DKO) mouse embryonic fibroblasts (MEFs) were grown in DMEM supplemented with 10% heat-inactivated FBS and 2 mM L-glutamine (Sigma) as described previously (20). The WNV 6-LP strain, previously established by plaque purification of the WNV NY99-6922 strain isolated from mosquitoes in 1999 (21,22), was kindly provided by Dr. Takashima (Hokkaido University, Japan). All experiments with WNV were performed at the Biosafety Level 3 facility at Hokkaido University in accordance with institutional guidelines. The influenza A virus (IFV) strain, A/Aichi/2/1968 (H3N2) was kindly provided by Dr. A. Takada (Hokkaido University, Japan).

**Antibodies and plasmids** – Rabbit anti-Japanese encephalitis virus serum was produced as described previously (23,24). Antibodies were purchased as follows: mouse anti-Rab8, anti-GM130 and anti-Rab11 monoclonal antibodies (BD Transduction Laboratories, San Diego, CA); mouse anti-WNV E protein and anti-actin monoclonal antibodies (Merck Millipore, Billerica, MA); rabbit anti-Rab5 polyclonal antibody and anti-Rab11 monoclonal antibody (Cell Signaling Technology, Beverly, MA); mouse anti-Rab11a monoclonal antibody, and rabbit anti-Lamp1 and anti-TGN46 polyclonal antibodies (Abcam, Cambridge, MA). Plasmid pCXS-N-Rab8b was constructed by subcloning PCR-amplified Rab8b from total RNA of Neuro 2a cells into pCXS-N, which was created by removing the myc-tag from pCMV-myc (Clontech) and adding *XhoI*, *Sall* and *NotI*

recognition site (25). WNV structural protein expressing plasmid (pCXSN-CME) was constructed as described previously (26,27). The WNV replicon cDNA constructs, pWNIrep-REN and pWNIrep-GFP, were generously provided by Dr. Robert W. Doms (17). A lentiviral vector pFU-pGK puro was generously provided by Dr. Kamitani (Osaka University, Japan), and the packaging plasmids (pCAF-HIVgp and pCMV-VSV-G-RSV-Rev) were generously provided by Dr. Miyoshi (Riken, Tsukuba, Japan).

*VLP release assay* – The validated siRNAs that target 18 Rab genes were purchased from Qiagen (Valencia, CA). HEK 293T cells were transfected with each siRNA by HiPerfect Transfection Reagent (Qiagen). At 48 hours, siRNA-transfected cells were transfected with WNV structural-protein-expressing plasmid (pCXSN-CME) and WNV replicon cDNA construct (pWNIrep-REN) that encode WNV nonstructural protein genes, and Renilla luciferase gene that is expressed instead of structural proteins (17), using Lipofectamine 2000 (Life Technologies, Rockville, MD). VLPs were released in culture supernatants and were unable to produce progeny particles because of a lack of structural protein genes in the replicon. Culture supernatants were harvested at 24 hours, and plasmid-transfected cells were lysed and measured for luciferase activity (transfection-associated luciferase activity) using the Dual Glo luciferase assay substrate (Promega, Madison, WI). Equal volumes of the harvested supernatants were used to infect Vero cells. VLP-infected cells were lysed and measured for luciferase activity (VLP-associated luciferase activity) at 60 hours post-infection (hpi). VLP release was calculated as ratio of luciferase activity of lysates of Vero cells/luciferase activity of 293T cells transfected with plasmids. The data were expressed as mean  $\pm$  SD. The Steel test was used for comparison. A value of  $p < 0.05$  was considered statistically significant.

*Immunoblotting* – For immunoblotting, cells were lysed in SDS-PAGE sample buffer supplemented with Complete Protease Inhibitor Cocktail (Roche Diagnostics, Indianapolis, IN). Cell lysates were fractionated by SDS-PAGE, and separated proteins were transferred to a PVDF filter (Merck

Millipore). The filter was incubated with each antibody, and the immune complexes were detected with HRP-conjugated secondary antibodies (Biosource International, Camarillo, CA) and Immobilon Western HRP-Substrate (Merck Millipore). The chemiluminescence signals were visualized with the VersaDoc 5000MP (Bio-Rad, Hercules, CA), and obtained images were analyzed using Quantity One software (Bio-Rad).

*Immunocytochemistry* – WNV-infected and mock-infected cells were fixed with 4% paraformaldehyde (PFA) for 10 minutes, before washing with PBS. The cells were permeabilized in 0.1% saponin or 0.1% Triton X-100 for 5 minutes, blocked with 1% BSA-PBS, and stained with indicated antibodies in 1% BSA-PBS overnight at 4°C. The immune complexes were visualized by incubating with Alexa-Fluor-488-, Alexa-Fluor-594- or Alexa-Fluor-647-conjugated secondary antibodies (Life Technologies). The cells were observed using a Zeiss 780 LSM confocal microscope (Carl Zeiss, Jena, Germany). For analysis of fluorescence intensity of viral antigen and number of GFP expressing cells, the cells were observed using an IN Cell Analyzer 2000 (GE Healthcare, Uppsala, Sweden), and obtained images were analyzed using IN Cell developer Toolbox software (GE Healthcare). For continuous transferrin internalization, WNV-infected cells were washed with Opti-MEM (Life Technologies) and incubated in Opti-MEM with 25  $\mu$ g/mL Alexa-Fluor-488-conjugated transferrin (Life Technologies) for 30 minutes at 37°C. Cells were washed twice with cold PBS and fixed with 4% PFA for 10 minutes. The signal of transferrin was observed using a Zeiss 780 LSM confocal microscope. Colocalization was analyzed using ZEN 2011 software (Carl Zeiss), and relative colocalization ratios were used as an indicator of colocalization as previously described (28). The ratio of the pixel number of colocalized viral proteins and each organelle marker to the whole pixel number was quantified by the confocal software ZEN 2011 and was represented by a bar graph. For quantification of colocalization, five cells from at least two independent experiments were used in each condition. The data were expressed as mean  $\pm$  SD. Student's *t*-test was used for comparison of obtained data.

**Plaque assay** – Diluted culture supernatants from infected cells were inoculated into monolayers of Vero cells. After 1 hour incubation at 37°C with rocking, the inocula were removed, and overlay medium (MEM containing 5% FBS and 1.25% methyl cellulose) was added and incubated for 4 days. Plaques were visualized with a 1% crystal violet solution in 70% ethanol.

**Ultracentrifugation** – For quantification of viral particle release, the culture supernatants were collected at 48 hpi and ultracentrifuged at 50,000 × *g* (SW28 rotor, Beckman Coulter, Brea, CA) at 20°C for 2 hours. The pellets were dissolved by PBS and analyzed by immunoblotting after addition of SDS-PAGE sample buffer.

**Influenza virus inoculation experiment** – WT and Rab8b KO MEFs were infected with IFV at 1 plaque-forming unit (Pfu)/cell and were cultured for 48 hours. The supernatants of IFV-infected MEFs were collected and incubated with 0.0005% acetylated trypsin (Sigma) at 37°C for 30 minutes. The incubated supernatants were transferred to MDCK cells. After 1 hour incubation at 37°C with rocking, the inocula were removed, and MEM containing 0.8% Bacto agar and 0.0005% acetylated trypsin was added and incubated for 2 days. Plaques were visualized with a 0.1% crystal violet solution in formalin.

**Rab11a and 11b knockdown (KD)** – The fragment was amplified by PCR, and subcloned into the pFU6-pGK puro vector, and the resulting plasmid was named pFU6-pGK puro shRab11a. 293T cells were transfected with pFU6-pGK puro shRab11a and the packaging plasmids using Polyethylenimine Max (Polysciences, Warrington, PA). After 48 hours, pseudotyped lentivirus bearing shRNA of Rab11a gene was harvested from the supernatant. WT and Rab8b KO MEFs were infected with the pseudotyped lentivirus and selected with puromycin for 1 week, and the resulting cells were named Rab11a KD WT MEFs and Rab11a KD Rab8b KO MEFs. For KD of Rab11b, the validated siRNA that targeted Rab11b gene was purchased from Qiagen. WT, Rab8b KO, Rab11a KD WT and Rab11a KD Rab8b KO MEFs were transfected with siRNA by Lipofectamine RNAi MAX (Life Technologies). At 24 hours,

siRNA-transfected cells were infected with WNV (1 Pfu/cell). Culture supernatants were harvested at 24 and 48 hours and viral titer was measured by plaque assay.

**Electron microscopy** – For ultrathin sections, WT and Rab8b KO MEFs infected with WNV at 1 Pfu/cell were cultured for 48 hours and were scraped off the plate, pelleted by centrifugation at 500 × *g* at 3 minutes, and fixed for 20 minutes with 2.5% glutaraldehyde in 0.1 M cacodylate buffer (pH 7.4). Small pieces of the fixed pellet were washed with cacodylate buffer, post-fixed with 2% osmium tetroxide in the cacodylate buffer for 1 hour at 4°C, dehydrated with a graded series of acetone, embedded in Epon 812 Resin mixture (TAAB Laboratories Equipment, Berks, UK), and polymerized at 60°C for 2 days. Ultrathin sections were stained with uranyl acetate and lead citrate and examined with a Hitachi H-7650 electron microscope (Tokyo, Japan).

## RESULTS

**Rab8b involved in WNV particle release** – We performed siRNA-based screening for silencing 18 Rab genes that are related to the vesicle transport from the ER to the plasma membrane to identify the Rab proteins associated with the later stages of WNV infection. We conducted a Renilla-luciferase-based virus assembly and release assay (Fig. 1A) as described previously (19). The gene-silenced 293T cells were co-transfected with plasmids expressing structural proteins (C, prM and E) and a subgenomic replicon that expressed the WNV nonstructural proteins and Renilla luciferase, resulted in the production of infectious VLPs in the culture fluid. Culture fluid was harvested at 24 hours post-transfection and cells were lysed and subjected to measurement of luciferase activity. To quantify the VLPs in the transfected culture fluid, Vero cells were inoculated with the harvested culture fluid, and then the luciferase activity of the Vero cells was measured at 60 hpi. Viral particle release was represented as ratio of luciferase activity of lysates of Vero cells/luciferase activity of 293T cells transfected with plasmids and replicon (Fig. 1A). The siRNA screen revealed that KD of Rab8b significantly decreased VLP release efficiency and KD of Rab27a significantly increased VLP release efficiency compared with

control siRNA-transfected cells (Fig. 1B).

KD of Rab8b inhibited secretion of WNV VLPs, and we further analyzed the role of Rab8b in WNV-infected cells. We examined the expression levels of Rab8 in WNV-infected human neuroblastoma SH-SY5Y cells. At 48 hpi, Rab8 expression level was increased in WNV-infected cells compared with mock-infected cells (Fig. 2A and B). We performed immunocytochemical analysis of Rab8 and the viral antigen in WNV-infected SH-SY5Y neuroblastoma cells. Immunopositive signals of Rab8 and the viral antigen were colocalized in the cytoplasm near the plasma membrane of WNV-infected cells (Fig. 2C, Rab8, arrowheads). WNV-infected SH-SY5Y cells were also examined by immunocytochemistry using antibodies against the viral antigen and various makers of endosomes, Golgi and other organelles. The viral antigen was colocalized with Rab11, a marker of recycling endosomes, at the perinuclear region (Fig. 2C, Rab11, arrowheads). We could not observe clear colocalization of the viral antigen and other organelle markers in SH-SY5Y cells (Rab5, Lamp1, GN130 and TGN46). Rab8 is localized to recycling endosomes and plays a role in vesicle transport to plasma membrane (11,29). Therefore, these results suggest that Rab8 plays an important role in release of WNV particles; probably from recycling endosomes to the plasma membrane.

#### *WNV antigens accumulate in Rab8b-deficient cells*

– To investigate the role of Rab8b in transport of WNV particles, Rab8b WT, Rab8b-deficient (Rab8b KO) and Rab8a and Rab8b (Rab8a+b)-deficient (DKO) MEFs were infected with WNV. We confirmed the expression levels of Rab8 in Rab8b KO and DKO MEFs by immunoblotting using an antibody, which recognized both Rab8a and Rab8b. The signal of Rab8a was observed in Rab8b KO MEFs and no signal of Rab8 was observed in DKO MEFs (Fig. 3A). We examined the efficiency of WNV replication among these cells. The viral titers in the culture supernatants from Rab8b KO and DKO MEFs were significantly lower than those of WT MEFs (Fig. 3B). This result is consistent with the observation that release of WNV-VLPs was significantly decreased by KD of Rab8b, but not KD of Rab8a (Fig. 1B). Although the expression level of E protein in the culture supernatant from

Rab8b KO MEFs was decreased compared with that from WT MEFs, the intracellular expression level of E protein in Rab8b KO MEFs was increased compared with that in WT MEFs (Fig. 3C). To examine whether re-expression of Rab8b in Rab8b KO MEFs rescued reduction of WNV replication, we complemented Rab8b KO MEFs with Rab8b. The Rab8b-complemented Rab8b KO MEFs were infected with WNV and the viral titer of the culture supernatants from the cells were examined. The signal intensity of Rab8a+b was increased in the Rab8b-transfected Rab8b KO MEFs compared that of mock-transfected Rab8b KO MEFs (Fig. 3D). The viral titers in the culture supernatants from Rab8b-transfected Rab8b KO MEFs were significantly higher compared with those from mock-transfected Rab8b KO MEFs at 48 hpi (Fig. 3E).

We examined the intracellular localization of E protein in WNV-infected WT and Rab8b KO MEFs. Confocal microscopic analysis revealed that E protein was present in the cytoplasm in a diffuse pattern in WT MEFs (Fig. 3F). However, the localization of E protein in Rab8b KO MEFs was distinct from that in WT MEFs, and it formed speckled spots in the cytoplasm (Fig. 3F). We also analyzed the fluorescence intensity of E protein in WNV-infected WT and Rab8b KO MEFs. The intensity of viral antigen in Rab8b KO MEFs was significantly higher than that in WT MEFs (Fig. 3G). These results suggest that Rab8b deficiency was associated with impaired release of viral proteins into the extracellular space and with accumulated viral proteins in the intracellular space.

To examine whether Rab8b affected the entry step of WNV infection, WT and Rab8b KO MEFs were infected with VLPs that possessed GFP-expressing WNV replicon RNA (17,26). VLPs are unable to produce progeny particles because of a lack of structural protein genes in the replicon (26). GFP positivity was analyzed by fluorescent microscopy and there were no significant difference of GFP positivity between WT and Rab8b KO MEFs (Fig. 3H). This result suggests that the Rab8b plays a role in post-entry steps in WNV infection.

To examine whether the reduction of viral titer in the supernatant of Rab8b-deficient cells was specific for WNV infection, the viral titers of the supernatants from IFV-infected WT and Rab8b

KO MEFs were examined. IFV buds at the plasma membrane (30). Unlike WNV infection, there was no significant difference in the viral titers of the supernatants from WT and Rab8b KO MEFs (Fig. 3I).

*WNV antigens accumulate in recycling endosomes in Rab8b deficient cells* – To identify the organelle that accumulated viral proteins, we analyzed the localization of viral protein and organelle markers in WT or Rab8b KO MEFs. The viral protein was partially colocalized with Rab11 and Rab8 in WT MEFs (Fig. 4A, upper columns, arrowheads). In contrast, the viral protein was accumulated in a speckled pattern and was markedly colocalized with Rab11 in Rab8b KO MEFs. The viral protein was colocalized with Rab8 in Rab8b KO MEFs (Fig. 4A, lower columns, arrowheads). Rab8a was expressed in Rab8b KO MEFs, therefore, this result indicates that the viral protein was localized at the Rab8a compartment. We also observed the colocalization of the viral protein and TGN46; a marker of the *trans*-Golgi at low frequency in WT MEFs. We also quantified the relative colocalization ratio of the viral protein and each organelle marker in WT and Rab8b KO MEFs. Compared with WT MEFs, the relative colocalization ratio of Rab11 was significantly higher in Rab8b KO MEFs (Fig. 4B). We further examined whether viral antigen accumulates in recycling endosomes in Rab8b KO MEFs. We incubated WT and Rab8b KO MEFs with Alexa-Fluor-488-conjugated transferrin, which accumulates recycling endosomes at 30 minutes after entry into the cells (31). Transferrin was mainly localized in the perinuclear region in mock-infected WT MEFs, whereas transferrin in mock-infected Rab8b KO MEFs was diffusely recognized in the cytoplasm (Fig. 4C). These results suggest that intracellular localization of recycling endosomes in MEFs is affected by knockout of Rab8b. Some viral protein was colocalized with internalized transferrin near the plasma membrane of WT MEFs (Fig. 4C, arrowheads), whereas the viral protein was highly colocalized with internalized transferrin in Rab8b KO MEFs (Fig. 4C, arrowheads). The viral antigen was colocalized with markers of recycling endosomes in both WT and Rab8b KO MEFs and the relative colocalization ratio was significantly higher in Rab8b KO MEFs. This suggests that

WNV commonly passes through the Rab11-positive recycling endosomes for their infection and that Rab8b plays a role in transport of WNV particles from recycling endosomes.

*Recycling endosomes are important for WNV replication* – We found that a large amount of viral protein was accumulated in recycling endosomes in Rab8b KO MEFs compared with WT MEFs (Fig. 4). To elucidate whether recycling endosomes are important for WNV transport, we examined the effect of both Rab11a and 11b depletion in WNV-inoculated WT and Rab8b KO MEFs. For depletion of Rab11a, we constructed recombinant lentivirus carrying shRNA. After lentivirus infection, Rab11 expression levels in both WT and Rab8b KO MEFs were decreased compared with control cells (Fig. 5A). Furthermore, Rab11b was depleted by siRNA specific for Rab11b in these cells. At 48 hours post-transfection, expression of Rab11 was markedly decreased (Fig. 5A). WT, Rab11a+b KD WT, Rab8b KO and Rab11a+b KD Rab8b KO MEFs were infected with WNV, and viral titers of the culture supernatants were examined. The viral titers of the supernatants from the Rab11a+b downregulated WT or Rab8b KO MEFs were significantly lower than those of the supernatants from the WT or Rab8b KO MEFs, respectively (Fig. 5B). These results suggest that intracellular trafficking through the Rab11-positive recycling endosomes is important for WNV replication.

*WNV particles accumulate in vesicles in Rab8b-deficient cells* – Transmission electron microscopy using Epon-embedded WNV-infected WT and Rab8b KO MEFs fixed at 48 hpi revealed many vesicular membrane structures (Ve in Fig. 6B and E), which are the viral genome replication site observed in flavivirus infection (32), and viral particles (Vi in Fig. 6B and E) in the proximity of the nucleus in both cells (Fig. 6A, B, D, E). The vesicles containing a few virus particles that were located distant from the viral replication site were observed in WT MEFs (Fig. 6C, white arrow heads). A large number of vesicles that contained many virus particles were observed in Rab8b KO MEFs (Fig. 6F, white arrow heads). The vesicular membrane structures were not observed in the vesicles, suggesting that these vesicles are a transport compartment and not the replication site.

These results suggest that viral particles are accumulated in the vesicles in the cytoplasm of Rab8b KO MEFs.

## DISCUSSION

In the present study, we showed that Rab8b was involved in regulation of the release of WNV particles from host cells. Rab8b deficiency resulted in accumulation of viral particles in the vesicles that were stained with recycling endosome markers at the cell periphery.

Rab8 participates in vesicular transport from the Golgi to the plasma membrane, particularly in transport from recycling endosomes to the plasma membrane (33,34). The two closely related proteins, Rab8a and Rab8b, which are encoded by different genes, are included in Rab8 (20). There are two possibilities about the function of Rab8b in WNV infection. First, viral particles are wrapped by Rab8b-positive vesicles and transported from recycling endosomes to the plasma membrane. Second, Rab8b-positive vesicles carry important molecules for viral transport from recycling endosomes. WNV antigen was colocalized with Rab8 and Rab11 in WNV-infected SH-SY5Y cells, suggesting that Rab8 plays a role in transport of vesicles containing WNV particles from recycling endosomes to the plasma membrane. The viral antigen and Rab8 double-positive sites were diffusely recognized in the cytoplasm, whereas the viral antigen and Rab11 double-positive sites were mainly recognized in the perinuclear region. The difference in intracellular localization of the viral antigen and organelle marker double-positive sites suggests that the viral antigen and Rab8 double-positive compartment is probably transport vesicles, but not recycling endosomes. Deficiency of Rab8b results in accumulation of viral particles in the recycling endosomes, supporting a model in which WNV particles bud from the recycling endosomes and are transported to the plasma membrane by Rab8b.

Dengue virus and Hantavirus exploit Rab8-related regulatory mechanisms for viral particle release (35-37). These viral particles, including WNV, assemble and bud into intracellular organelles, such as the ER or Golgi apparatus, and are transported by vesicular trafficking to the plasma membrane (10,37). In contrast, the release of IFV, which has a different

release mechanism from that of WNV, was not affected by Rab8b deficiency. Rab8 may have common roles in release of viral particles that have budded in the intracellular organelles. Regarding WNV particle release, an apparent contradiction was observed in previous findings that WNV particles were released from the apical surface (38), or released from the basolateral side (27,39). A large number of intracellular sorting mechanisms occurring in virus-infected cells have been proposed. Rab8a is associated with apical transport, while Rab8b functions in basolateral transport (20,29,40). In our current study, KD of Rab8a had no significant effect on the release of viral particles, whereas KD of Rab8b inhibited particle release. These results suggest that WNV particles are released from the basolateral side.

Following maturation of WNV particles in the *trans*-Golgi network, viral particles are sorted into secretory vesicles and are transported to the plasma membrane (9,10). Rab11a-positive recycling endosomes sort some vesicles to define the directions during exocytosis (41,42). Hepatitis C virus particles are localized in recycling endosomes transiently and the recycling endosomes serve as a sorting station (43). We found that WNV particles colocalized with Rab11- and transferrin-positive recycling endosomes in infected cells. This result suggests that the transit of vesicles containing viral particles to recycling endosomes is a general mechanism for the release of *Flaviviridae* viruses. Moreover, we noticed that Rab11- and transferrin-positive recycling endosomes were localized near the plasma membrane in Rab8b KO cells. Endogenous recycling endosomes are distributed throughout the cytoplasm, and relatively concentrated in the perinuclear region (42). However, in Rab11 interaction factors, such as Sec15 or Exo70, KD cells, Rab11-positive recycling endosomes are found near the plasma membrane (42). Our results suggest that Rab8b interacts with Rab11 during secretion of WNV particles. Although WNV replication was significantly decreased by co-depletion of Rab11a and Rab11b, downregulation of Rab11a or Rab11b showed no significant difference in the release of viral particles. These results suggest that there is functional redundancy between Rab11a and Rab11b in the particle release pathway.

Rab27a and Rab27b are regulatory factors of



secretion of exosomes (44), and Rab27a dysfunction is related to the cause of human immunodeficiency (45). Interferon- $\alpha$ -stimulated cells induce exosomes that can carry antiviral molecules (46). Increase of VLP release in Rab27a KD cells might be related to inhibition of release of exosomes carrying antiviral molecules. This phenomenon needs to be clarified.

In conclusion, this study provides new information about the release pathway of WNV

particles that egress from cells, depending on the function of Rab8b, through recycling endosomes. As demonstrated by the influenza virus inhibitors, the understanding about the processes of viral particle release and budding will provide important information for development of therapeutic strategies. Further investigation of the detailed mechanism of transport and release of the viral particles is necessary.

**Acknowledgments:** We would like to thank Dr. Takashima for providing the WNV NY99 6-LP strain; Dr. Doms for the WNV replicon cDNA construct pWNIrep-GFP; Dr. Kamitani for providing the pFU-pGK puro; Dr. Miyoshi for providing the lentiviral packaging plasmids (pCAG-HIVgp and pCMV-VSV-G-RSV-Rev) and all members of the Sawa Laboratory for helpful discussion. We are especially grateful for the experimental assistance and advice of Dr. Yamasaki, Dr. Muramatsu and Mr. Maruyama.

**Conflict of interest:** The authors declare that they have no conflict of interests with the contents of this article.

**Author contributions:** SK, TS and HS conceived and designed the study. SK, TS, AK and WP performed the experiments and data analysis. SK, KY, HK, YO and HS wrote the paper. TI and AH provided critical reagents.

## REFERENCES

1. Hayes, E. B., Sejvar, J. J., Zaki, S. R., Lanciotti, R. S., Bode, A. V., and Campbell, G. L. (2005) Virology, pathology, and clinical manifestations of West Nile virus disease. *Emerg Infect Dis* **11**, 1174-1179
2. Guarner, J., Shieh, W. J., Hunter, S., Paddock, C. D., Morken, T., Campbell, G. L., Marfin, A. A., and Zaki, S. R. (2004) Clinicopathologic study and laboratory diagnosis of 23 cases with West Nile virus encephalomyelitis. *Hum Pathol* **35**, 983-990
3. Brinton, M. A. (2002) The molecular biology of West Nile Virus: a new invader of the western hemisphere. *Annu Rev Microbiol* **56**, 371-402
4. Samuel, M. A., and Diamond, M. S. (2006) Pathogenesis of West Nile Virus infection: a balance between virulence, innate and adaptive immunity, and viral evasion. *J Virol* **80**, 9349-9360
5. Suthar, M. S., Diamond, M. S., and Gale, M. (2013) West Nile virus infection and immunity. *Nat Rev Microbiol* **11**, 115-128
6. Fernandez-Garcia, M. D., Mazzon, M., Jacobs, M., and Amara, A. (2009) Pathogenesis of flavivirus infections: using and abusing the host cell. *Cell Host Microbe* **5**, 318-328
7. Gillespie, L. K., Hoenen, A., Morgan, G., and Mackenzie, J. M. (2010) The endoplasmic reticulum provides the membrane platform for biogenesis of the flavivirus replication complex. *J Virol* **84**, 10438-10447
8. Murray, C. L., Jones, C. T., and Rice, C. M. (2008) Architects of assembly: roles of Flaviviridae non-structural proteins in virion morphogenesis. *Nat Rev Microbiol* **6**, 699-708
9. Mackenzie, J. M., and Westaway, E. G. (2001) Assembly and maturation of the flavivirus Kunjin virus appear to occur in the rough endoplasmic reticulum and along the secretory pathway, respectively. *J Virol* **75**, 10787-10799
10. Mukhopadhyay, S., Kuhn, R. J., and Rossmann, M. G. (2005) A structural perspective of the

- flavivirus life cycle. *Nat Rev Microbiol* **3**, 13-22
11. Henry, L., and Sheff, D. R. (2008) Rab8 regulates basolateral secretory, but not recycling, traffic at the recycling endosome. *Mol Biol Cell* **19**, 2059-2068
  12. Chen, S., Liang, M. C., Chia, J. N., Ngsee, J. K., and Ting, A. E. (2001) Rab8b and its interacting partner TRIP8b are involved in regulated secretion in AtT20 cells. *J Biol Chem* **276**, 13209-13216
  13. Guichard, A., Nizet, V., and Bier, E. (2014) RAB11-mediated trafficking in host-pathogen interactions. *Nat Rev Microbiol* **12**, 624-634
  14. Krishnan, M. N., Sukumaran, B., Pal, U., Agaisse, H., Murray, J. L., Hodge, T. W., and Fikrig, E. (2007) Rab 5 is required for the cellular entry of dengue and West Nile viruses. *J Virol* **81**, 4881-4885
  15. Krishnan, M. N., Ng, A., Sukumaran, B., Gilfoy, F. D., Uchil, P. D., Sultana, H., Brass, A. L., Adametz, R., Tsui, M., Qian, F., Montgomery, R. R., Lev, S., Mason, P. W., Koski, R. A., Elledge, S. J., Xavier, R. J., Agaisse, H., and Fikrig, E. (2008) RNA interference screen for human genes associated with West Nile virus infection. *Nature* **455**, 242-245
  16. Ooi, Y. S., Stiles, K. M., Liu, C. Y., Taylor, G. M., and Kielian, M. (2013) Genome-wide RNAi screen identifies novel host proteins required for alphavirus entry. *PLoS Pathog* **9**, e1003835
  17. Pierson, T. C., Sánchez, M. D., Puffer, B. A., Ahmed, A. A., Geiss, B. J., Valentine, L. E., Altamura, L. A., Diamond, M. S., and Doms, R. W. (2006) A rapid and quantitative assay for measuring antibody-mediated neutralization of West Nile virus infection. *Virology* **346**, 53-65
  18. Puig-Basagoiti, F., Deas, T. S., Ren, P., Tilgner, M., Ferguson, D. M., and Shi, P. Y. (2005) High-throughput assays using a luciferase-expressing replicon, virus-like particles, and full-length virus for West Nile virus drug discovery. *Antimicrob Agents Chemother* **49**, 4980-4988
  19. Garg, H., Lee, R. T., Tek, N. O., Maurer-Stroh, S., and Joshi, A. (2013) Identification of conserved motifs in the West Nile virus envelope essential for particle secretion. *BMC Microbiol* **13**, 197
  20. Sato, T., Iwano, T., Kunii, M., Matsuda, S., Mizuguchi, R., Jung, Y., Hagiwara, H., Yoshihara, Y., Yuzaki, M., Harada, R., and Harada, A. (2014) Rab8a and Rab8b are essential for several apical transport pathways but insufficient for ciliogenesis. *J Cell Sci* **127**, 422-431
  21. Shirato, K., Kimura, T., Mizutani, T., Kariwa, H., and Takashima, I. (2004) Different chemokine expression in lethal and non-lethal murine West Nile virus infection. *J Med Virol* **74**, 507-513
  22. Shirato, K., Miyoshi, H., Goto, A., Ako, Y., Ueki, T., Kariwa, H., and Takashima, I. (2004) Viral envelope protein glycosylation is a molecular determinant of the neuroinvasiveness of the New York strain of West Nile virus. *J Gen Virol* **85**, 3637-3645
  23. Kimura, T., Kimura-Kuroda, J., Nagashima, K., and Yasui, K. (1994) Analysis of virus-cell binding characteristics on the determination of Japanese encephalitis virus susceptibility. *Arch Virol* **139**, 239-251
  24. Kobayashi, S., Orba, Y., Yamaguchi, H., Kimura, T., and Sawa, H. (2012) Accumulation of ubiquitinated proteins is related to West Nile virus-induced neuronal apoptosis. *Neuropathology* **32**, 398-405
  25. Kobayashi, S., Suzuki, T., Igarashi, M., Orba, Y., Ohtake, N., Nagakawa, K., Niikura, K., Kimura, T., Kasamatsu, H., and Sawa, H. (2013) Cysteine residues in the major capsid protein, Vp1, of the JC virus are important for protein stability and oligomer formation. *PLoS One* **8**, e76668
  26. Kobayashi, S., Orba, Y., Yamaguchi, H., Takahashi, K., Sasaki, M., Hasebe, R., Kimura, T., and Sawa, H. (2014) Autophagy inhibits viral genome replication and gene expression stages in West Nile virus infection. *Virus Res* **191**, 83-91
  27. Hasebe, R., Suzuki, T., Makino, Y., Igarashi, M., Yamanouchi, S., Maeda, A., Horiuchi, M., Sawa, H., and Kimura, T. (2010) Transcellular transport of West Nile virus-like particles across human endothelial cells depends on residues 156 and 159 of envelope protein. *BMC Microbiol* **10**, 165
  28. de Kreuk, B. J., Anthony, E. C., Geerts, D., and Hordijk, P. L. (2012) The F-BAR protein PACSIN2 regulates epidermal growth factor receptor internalization. *J Biol Chem* **287**, 43438-43453

29. Ang, A. L., Fölsch, H., Koivisto, U. M., Pypaert, M., and Mellman, I. (2003) The Rab8 GTPase selectively regulates AP-1B-dependent basolateral transport in polarized Madin-Darby canine kidney cells. *J Cell Biol* **163**, 339-350
30. Noda, T., Sagara, H., Yen, A., Takada, A., Kida, H., Cheng, R. H., and Kawaoka, Y. (2006) Architecture of ribonucleoprotein complexes in influenza A virus particles. *Nature* **439**, 490-492
31. Ullrich, O., Reinsch, S., Urbé, S., Zerial, M., and Parton, R. G. (1996) Rab11 regulates recycling through the pericentriolar recycling endosome. *J Cell Biol* **135**, 913-924
32. Welsch, S., Miller, S., Romero-Brey, I., Merz, A., Bleck, C. K., Walther, P., Fuller, S. D., Antony, C., Krijnse-Locker, J., and Bartenschlager, R. (2009) Composition and three-dimensional architecture of the dengue virus replication and assembly sites. *Cell Host Microbe* **5**, 365-375
33. Knödler, A., Feng, S., Zhang, J., Zhang, X., Das, A., Peränen, J., and Guo, W. (2010) Coordination of Rab8 and Rab11 in primary ciliogenesis. *Proc Natl Acad Sci U S A* **107**, 6346-6351
34. Das, A., and Guo, W. (2011) Rabs and the exocyst in ciliogenesis, tubulogenesis and beyond. *Trends Cell Biol* **21**, 383-386
35. Xu, X. F., Chen, Z. T., Zhang, J. L., Chen, W., Wang, J. L., Tian, Y. P., Gao, N., and An, J. (2008) Rab8, a vesicular traffic regulator, is involved in dengue virus infection in HepG2 cells. *Intervirology* **51**, 182-188
36. Xu, X. F., Chen, Z. T., Gao, N., Zhang, J. L., and An, J. (2009) Myosin Vc, a member of the actin motor family associated with Rab8, is involved in the release of DV2 from HepG2 cells. *Intervirology* **52**, 258-265
37. Rowe, R. K., Suszko, J. W., and Pekosz, A. (2008) Roles for the recycling endosome, Rab8, and Rab11 in hantavirus release from epithelial cells. *Virology* **382**, 239-249
38. Chu, J. J., and Ng, M. L. (2002) Infection of polarized epithelial cells with flavivirus West Nile: polarized entry and egress of virus occur through the apical surface. *J Gen Virol* **83**, 2427-2435
39. Verma, S., Lo, Y., Chapagain, M., Lum, S., Kumar, M., Gurjav, U., Luo, H., Nakatsuka, A., and Nerurkar, V. R. (2009) West Nile virus infection modulates human brain microvascular endothelial cells tight junction proteins and cell adhesion molecules: Transmigration across the in vitro blood-brain barrier. *Virology* **385**, 425-433
40. Sato, T., Mushiake, S., Kato, Y., Sato, K., Sato, M., Takeda, N., Ozono, K., Miki, K., Kubo, Y., Tsuji, A., Harada, R., and Harada, A. (2007) The Rab8 GTPase regulates apical protein localization in intestinal cells. *Nature* **448**, 366-369
41. Yu, S., Nie, Y., Knowles, B., Sakamori, R., Stypulkowski, E., Patel, C., Das, S., Douard, V., Ferraris, R. P., Bonder, E. M., Goldenring, J. R., Ip, Y. T., and Gao, N. (2014) TLR sorting by Rab11 endosomes maintains intestinal epithelial-microbial homeostasis. *EMBO J* **33**, 1882-1895
42. Takahashi, S., Kubo, K., Waguri, S., Yabashi, A., Shin, H. W., Katoh, Y., and Nakayama, K. (2012) Rab11 regulates exocytosis of recycling vesicles at the plasma membrane. *J Cell Sci* **125**, 4049-4057
43. Collier, K. E., Heaton, N. S., Berger, K. L., Cooper, J. D., Saunders, J. L., and Randall, G. (2012) Molecular determinants and dynamics of hepatitis C virus secretion. *PLoS Pathog* **8**, e1002466
44. Ostrowski, M., Carmo, N. B., Krumeich, S., Fanget, I., Raposo, G., Savina, A., Moita, C. F., Schauer, K., Hume, A. N., Freitas, R. P., Goud, B., Benaroch, P., Hacoheh, N., Fukuda, M., Desnos, C., Seabra, M. C., Darchen, F., Amigorena, S., Moita, L. F., and Thery, C. (2010) Rab27a and Rab27b control different steps of the exosome secretion pathway. *Nat Cell Biol* **12**, 19-30; sup pp 11-13
45. Fukuda, M. (2005) Versatile role of Rab27 in membrane trafficking: focus on the Rab27 effector families. *J Biochem* **137**, 9-16
46. Li, J., Liu, K., Liu, Y., Xu, Y., Zhang, F., Yang, H., Liu, J., Pan, T., Chen, J., Wu, M., Zhou, X., and Yuan, Z. (2013) Exosomes mediate the cell-to-cell transmission of IFN- $\alpha$ -induced antiviral activity. *Nat Immunol* **14**, 793-803

**FOOTNOTES**

This study was supported in part by JSPS KAKENHI Grant Number 15K19069 and grants from the Ministry of Education, Culture, Sports, Science and Technology of Japan (MEXT); the Ministry of Health, Labour and Welfare of Japan; and the Japan Initiative for Global Research Network on Infectious Diseases (J-GRID); as well as by the Grant from MEXT for Joint Research Program of the Research Center for Zoonosis Control, Hokkaido University.

The abbreviations used are: ER, endoplasmic reticulum; hpi, hours post-infection; IFV, Influenza A virus; KD, knockdown; MEF, mouse embryonic fibroblast; MEM, minimal essential medium; PFA: paraformaldehyde; Pfu, plaque-forming unit; VLP, virus-like particle; WNV, West Nile virus

**FIGURE 1.** siRNA screen for WNV particle release. (A) Strategy of siRNA screening. siRNAs were introduced into 293T cells, and these cells were transfected with plasmids expressing WNV structural proteins (C, prM and E) and replicon. Vero cells were inoculated with the harvested culture fluid containing VLPs. The plasmids-transfected 293T cells and VLPs-infected Vero cells were harvested, and the luciferase activities were measured. (B) Quantification of released VLPs from siRNA-transfected 293T cells. VLP release efficiency was calculated as the ratio of luciferase activity of Vero cells/luciferase activity of 293T cells. Data represent mean  $\pm$  SD of three independent experiments. Statistical significance was assessed using the Steel test, and is indicated by asterisks ( $*p < 0.05$ ).

**FIGURE 2.** Rab8 expression and localization are controlled by WNV infection. (A) Rab8 expression levels in WNV-infected cells. SH-SY5Y cells were mock-infected (Mock) or infected with WNV (1 Pfu/cell). Cells were harvested at 48 hpi and analyzed by immunoblotting for Rab8, E protein and actin. (B) Quantified result of (A). The bar graph represents relative Rab8 band densities that were normalized for actin band densities. Data represent mean  $\pm$  SD of three independent experiments. (C) Intracellular localization of viral protein and each organelle marker. SH-SY5Y cells were mock-infected (Mock) or infected with WNV (1 Pfu/cell). Cells were harvested at 48 hpi and stained with each organelle marker (green) and WNV antigen (red). Cell nuclei were counterstained with DAPI (blue). Arrowheads indicate colocalization of viral antigen and each organelle marker. Scale bars: 5  $\mu$ m. Boxed areas in Rab8 and Rab11 were magnified in right panels.

**FIGURE 3.** Viral protein is accumulated in cytoplasm in Rab8b KO MEFs. (A) Rab8 expression levels in WT, Rab8 KO or DKO MEFs. WT, Rab8b KO or DKO MEFs were analyzed by immunoblotting for Rab8 and actin. (B) Viral titer in culture supernatants. WT, Rab8b KO and DKO MEFs were infected with WNV (1 Pfu/cell). Culture supernatants were harvested at 48 hpi and viral titers were determined by the plaque assay. Data represent mean  $\pm$  SD of three independent experiments. Statistical significance was assessed using Student's *t*-test, and is indicated by asterisks ( $**p < 0.01$ ). (C) Comparison of amount of E protein. Culture supernatants (SUP) and whole cell lysates (WCL) from WNV-infected WT or Rab8b KO MEFs were analyzed by immunoblotting for E protein, Rab8 and actin. These cells were prepared at 48 hpi. (D) Rab8a+b expression levels of Rab8b-complemented Rab8b KO MEFs. Control plasmid (Mock) or Rab8b expression plasmid (Rab8b) was introduced into WT or Rab8b KO MEFs, thereafter transfected cells were analyzed by immunoblotting for Rab8 and actin. (E) Viral titer in culture supernatants from control- or Rab8b expression plasmid-transfected Rab8b KO MEFs. After 24 hours, plasmid-transfected cells were infected with WNV (1 Pfu/cell). Culture supernatants were harvested at 48 hpi, and viral titers were measured by plaque assay. Data represent mean  $\pm$  SD of three independent experiments. Statistical significance was assessed using Student's *t*-test, and is indicated by asterisks ( $**p < 0.01$ ). (F) Intracellular localization of E protein. WT or Rab8b KO MEFs were infected with WNV (1 Pfu/cell). Cells were harvested at 48 hpi and stained with E protein (green). Cell nuclei were counterstained with DAPI (blue). Scale bars: 10  $\mu$ m. (G) Fluorescence intensity of viral antigen. WNV-infected WT or Rab8b KO MEFs were harvested at 48 hpi and stained with viral antigen. Fluorescence intensity of viral antigen in each cell was analyzed by IN Cell Analyzer. Data represent mean  $\pm$  SD of three independent experiments. Statistical significance was assessed using the Student's *t*-test, and is indicated by asterisks ( $**p < 0.01$ ). (H) Rab8b does not influence the entry step of WNV infection. WT or Rab8b KO MEFs were inoculated with the VLPs encoding GFP, and GFP positivity was measured by IN Cell Analyzer. Data represent mean  $\pm$  SD of three independent experiments. Statistical significance was assessed using the Student's *t*-test. (I) Rab8b does not affect replication of IFV. WT or Rab8b KO MEFs were inoculated with the IFV (1Pfu/cell). The culture supernatants were harvested at 24 hpi and viral titers were measured by plaque assay. Data represent mean  $\pm$  SD of three independent experiments. Statistical significance was assessed using Student's *t*-test.

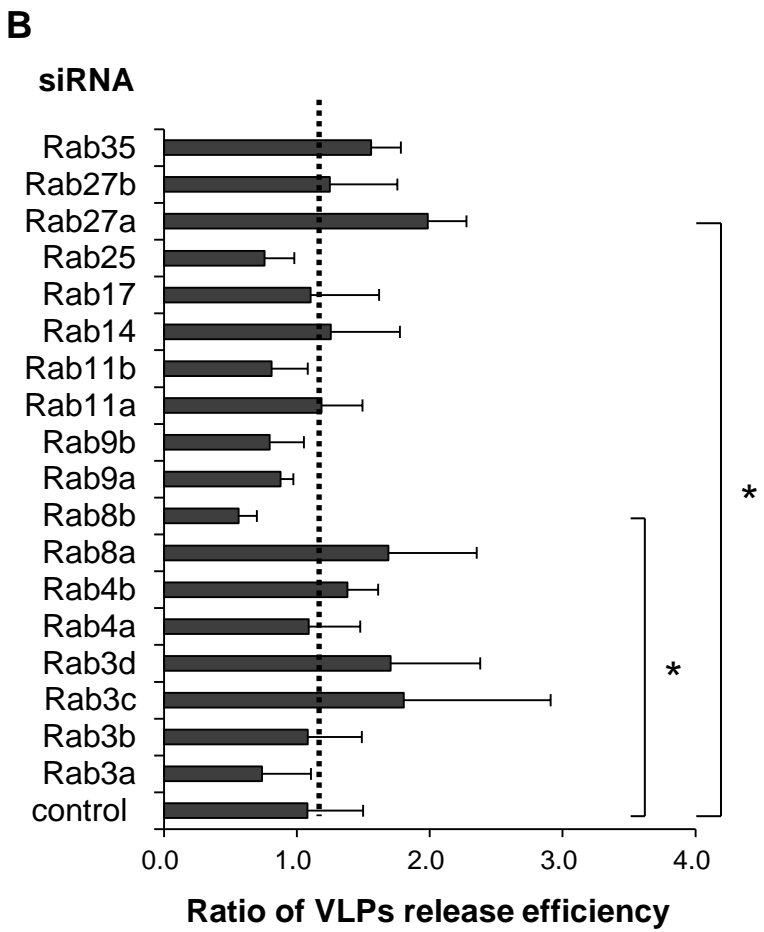
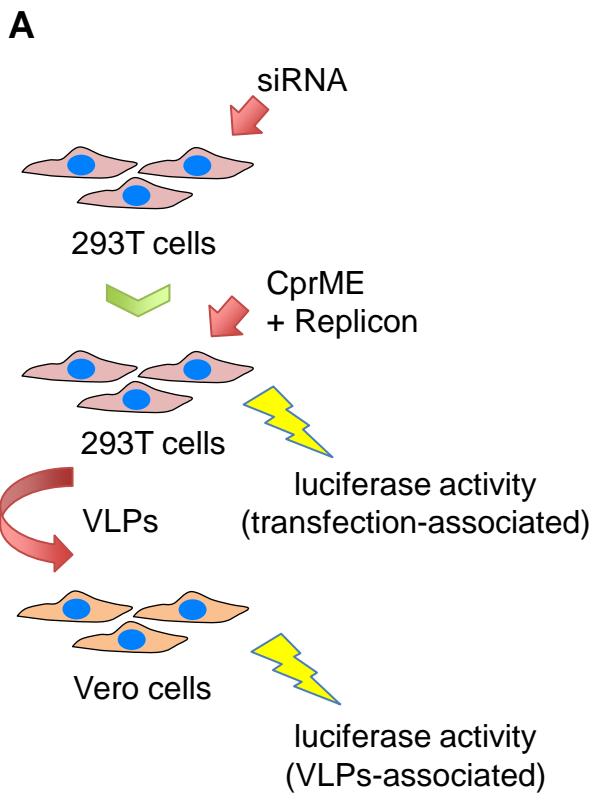
**FIGURE 4.** Viral protein is accumulated in recycling endosomes in Rab8b KO MEFs. (A) Intracellular localization of viral protein. WT or Rab8b KO MEFs were infected with WNV (1 Pfu/cell). Cells were

harvested at 48 hpi and stained with viral protein (red) and organelle markers (green). Cell nuclei were counterstained with DAPI (blue). Arrowheads indicate colocalization of viral antigen and each organelle marker. Scale bars: 5  $\mu$ m. Boxed areas in Rab11, TGN46 and Rab8 were magnified in right panels. (B) Quantification of colocalization of each organelle marker and viral antigen. The ratio of pixel number of colocalized viral proteins and each organelle marker to the whole pixel number was quantified by confocal software ZEN 2011 and is represented by a bar graph. Data represent mean  $\pm$  SD of three independent experiments. Statistical significance was assessed using Student's *t*-test, and is indicated by asterisks ( $*p < 0.05$ ). (C) Localization of transferrin and viral antigen. WNV-infected cells were incubated with Alexa-Fluor-488-conjugated transferrin (green). Cells were harvested and stained with viral antigen (red). Cell nuclei were counterstained with DAPI (blue). Scale bars: 5  $\mu$ m. Boxed areas were magnified in right panels. Arrowheads indicate colocalization of transferrin and viral antigen.

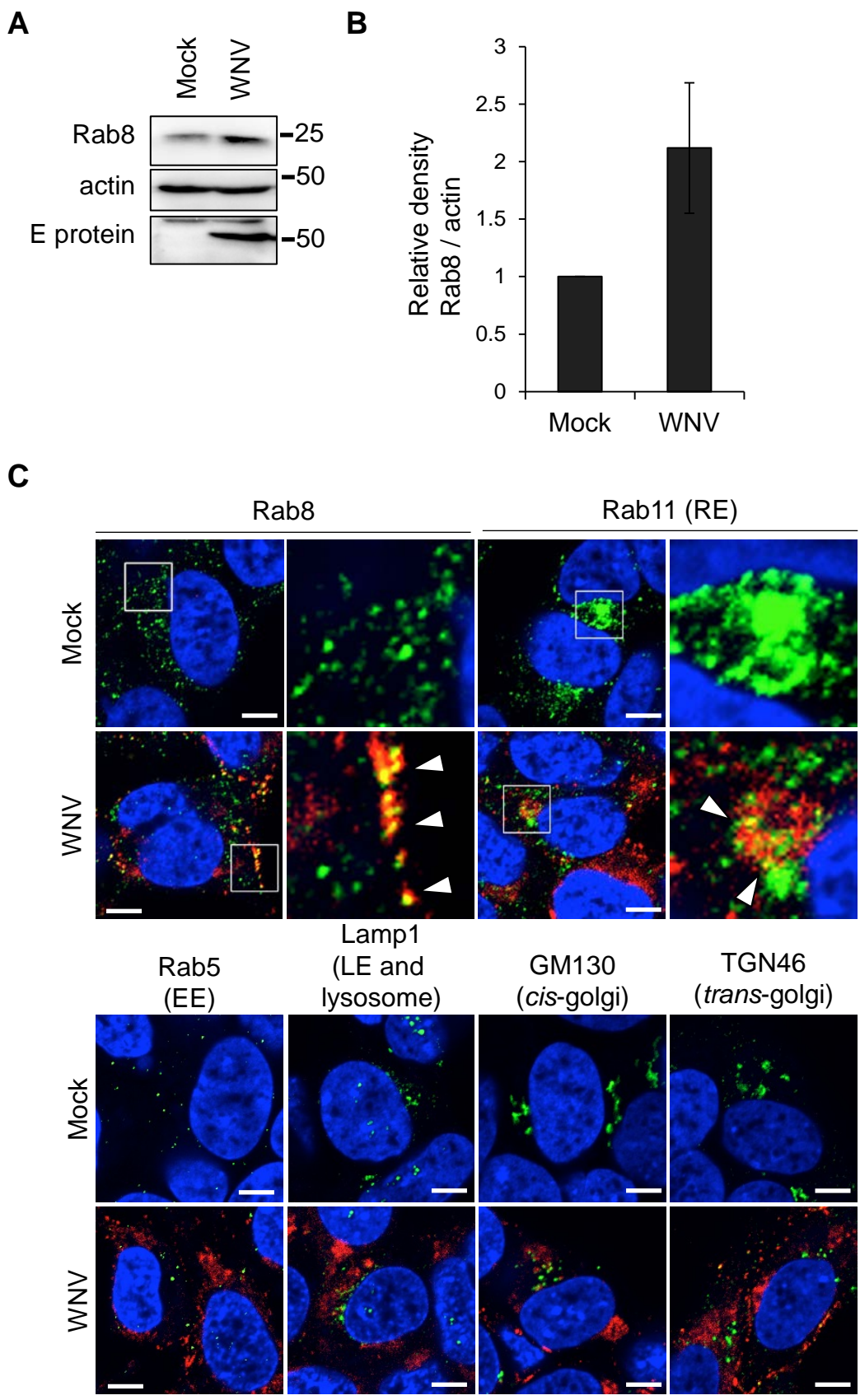
**FIGURE 5.** Rab11 plays an important role for WNV replication. (A) Rab11 expression levels in Rab11 KD cells. WT or Rab8b KO MEFs were infected with recombinant lentivirus carrying shRNA against mouse Rab11a expression cassette (Rab11a KD). shRNA transduced MEFs were transfected with siRNA against mouse Rab11b (Rab11a+b KD). These cells were analyzed by immunoblotting for Rab11 and actin. (B) Viral titer in culture supernatants of WT, Rab11a/b KD WT, Rab8b KO and Rab11a+b KD Rab8b KO MEFs. After 24 hours, siRNA-transfected cells were infected with WNV (1 Pfu/cell), culture supernatants were harvested at 48 hpi, and viral titers were measured by plaque assay. Data represent mean  $\pm$  SD of three independent experiments. Statistical significance was assessed using Student's *t*-test.

**FIGURE 6.** Ultrastructural analysis of WNV-infected WT or Rab8b KO MEFs. Ultrathin sections of WNV-infected, Epon-embedded WT or Rab8b MEFs fixed at 48 hpi are shown in (A–C) or (D–F), respectively. The red and white-boxed areas in (A) are shown at higher magnification in (B) and (C), respectively. The red and white-boxed areas in (D) are shown at higher magnification in (E) and (F), respectively. Arrowheads in (C) and (F) indicate vesicles containing viral particles. Scale bars: 200 nm.

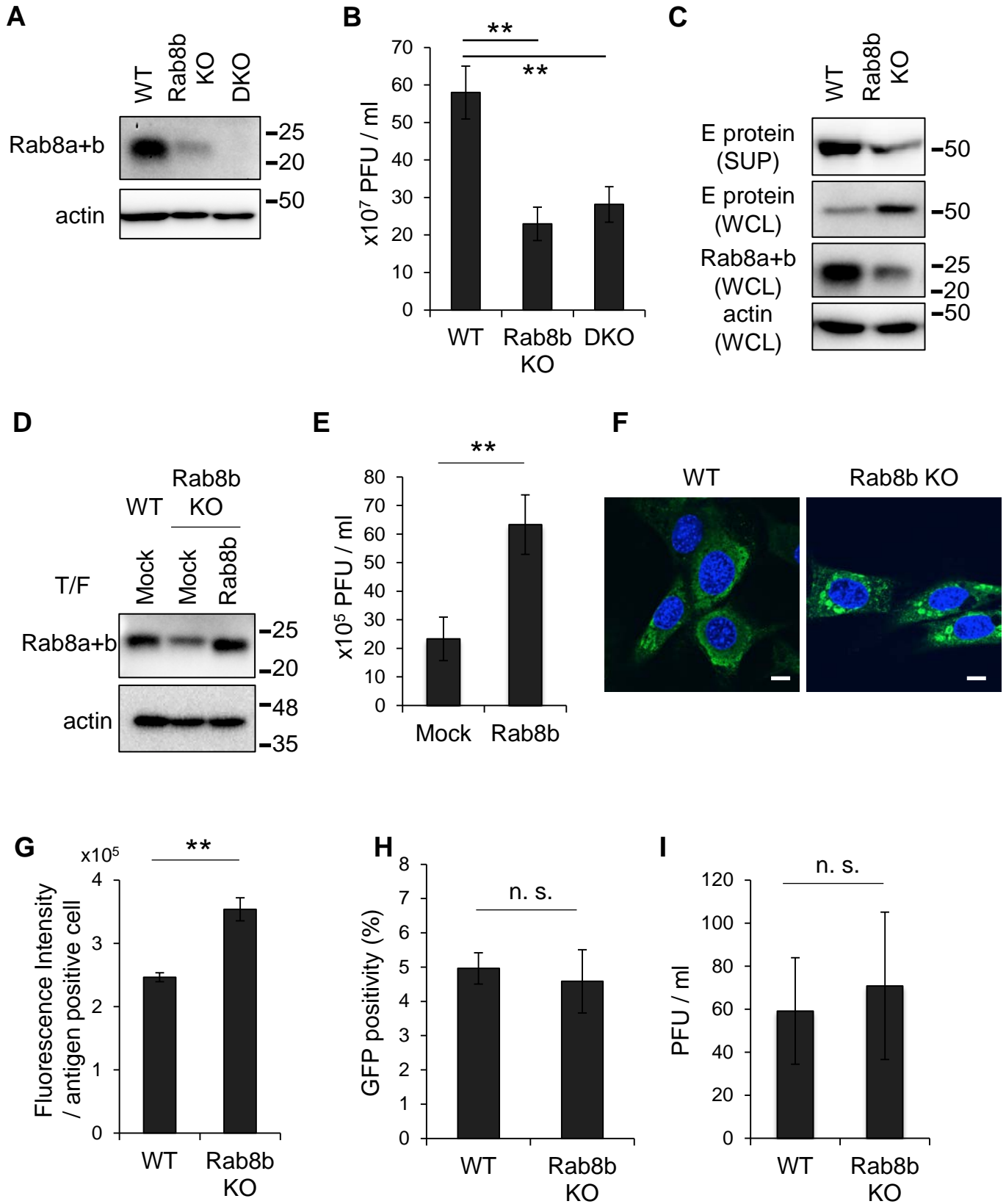
# Fig. 1



# Fig. 2

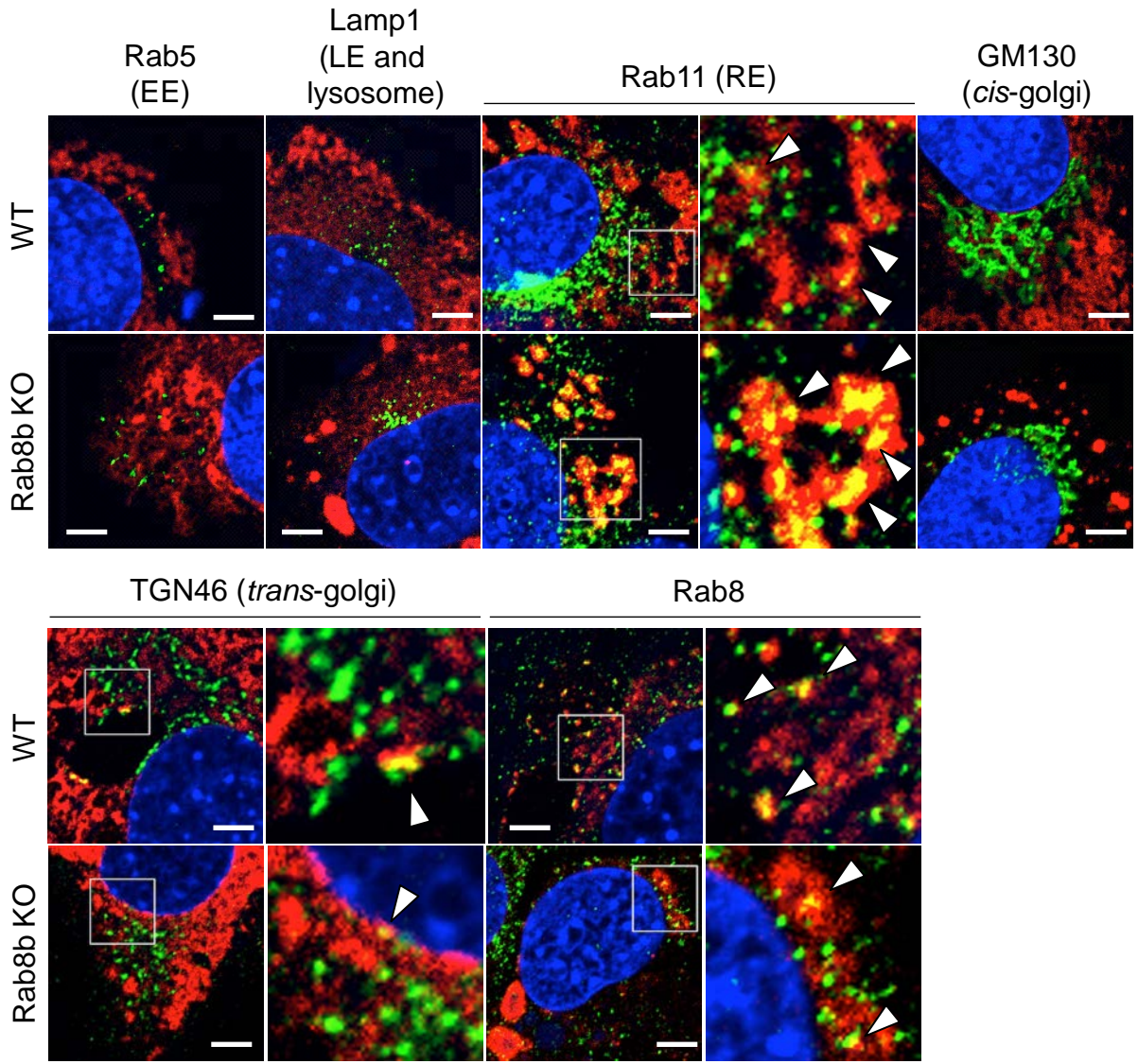




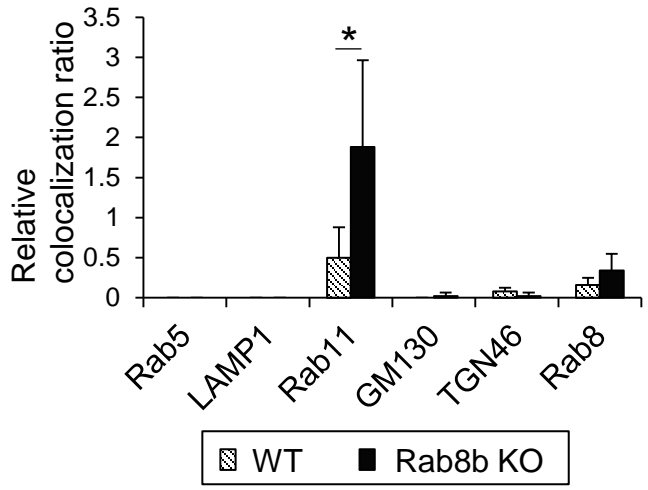
**Fig. 3**

# Fig. 4

**A**



**B**



**C**

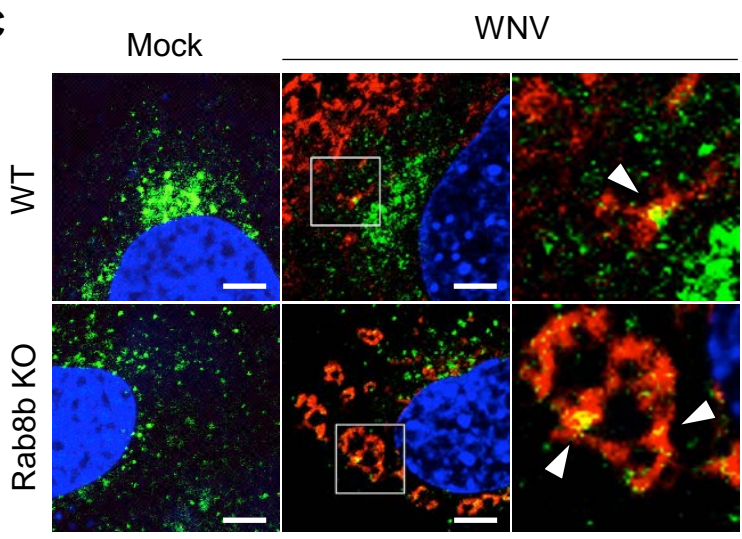


**Fig. 5**

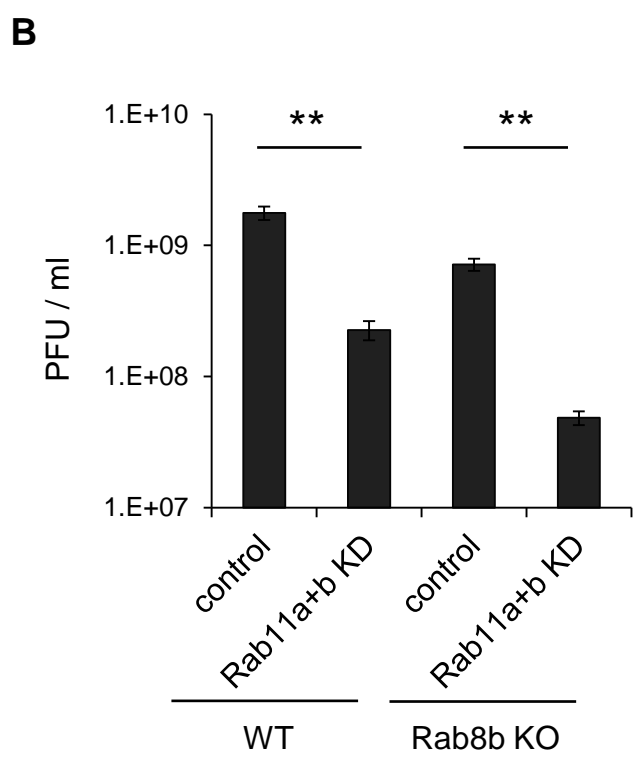
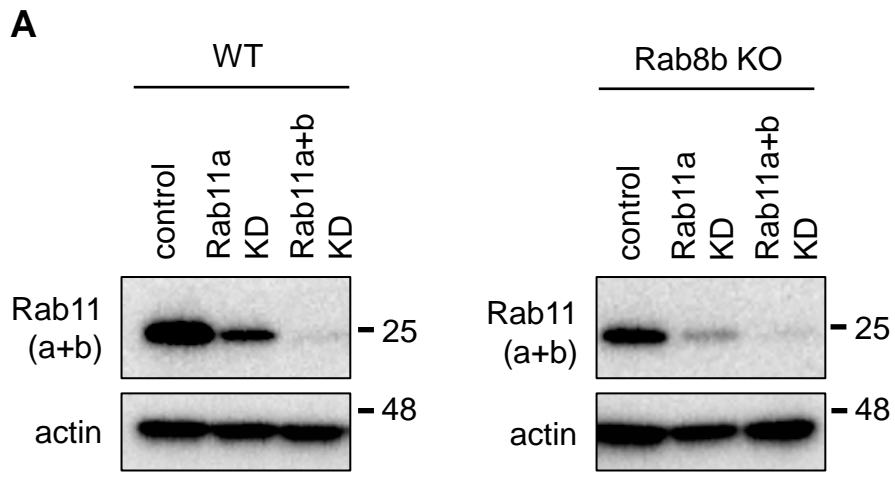




**Fig. 6**

